Development of a compact regenerative braking system for electric vehicles

Giannis Tzortzis[1], Amargianos Alexandros[2], Savvas Piperidis[3*],
Eftichios Koutroulis[4] and Nikos C. Tsourveloudis[5]

Abstract— In this paper, a detailed study and implementation of a reliable and efficient regenerative braking system is presented. It is applied on a prototype electric vehicle, that uses a hydrogen fuel cell as its only power source. Supercapacitors are used to store the energy that is generated during braking, transistors for switching the alternative circuits and an embedded computer controller program undertakes the synchronization of the system tasks. A finite state machine was designed to create a simple but robust technique to control the transistor switches according to the system's sensory inputs. The system is powered by its own supercapacitors, and thus it may be used in a plug-and-play manner. On-road test drives proved the system's reliability and efficiency.

I. INTRODUCTION

Nowadays, more than ever, the use of oil, natural gas and other fossil fuels as power source for the automotive vehicles equipped with internal combustion engines (ICE), exposes its important drawbacks opposed to the use of electricity at the electric vehicles (EV):

1) The global fossil fuels reserves are finite. Instead, the use of electricity, produced by renewable energy sources (RES) [1], [2] and stored chemically in some medium like hydrogen or batteries is a, long term, environmentally friendly, cost-effective, zero-emission solution for *endless* automotive power supply.

2) There are geopolitical and economical impacts due to the existence of fossil fuels exclusively at just a few locations around the world. However, this is not the case with the RES, being available almost everywhere around the world.

3) ICE operation is noisy while electric motors run silently. ICE operation, also, pollutes air with exhaust gases, like carbon dioxide and intensify the universal greenhouse effect problem. Moreover, ICE need lubrication and the used, toxic and contaminant lubricants should be properly recycled at given intervals. On the other hand, electricity and electric motors do not produce any kind of *dirty* gases [1] or contaminated

disposals. Finally, ICE efficiency in commecial vehicles is around 30% [3] while contemporary electric motors present efficiency up to 95% [4].

The use of hybrid techniques at EVs equipped with two or more different electric power sources improves efficiency, paying on the other hand the price of a higher level of complexity [5]–[8]. Hybrid design offers the potential of exploiting, in the sense of collecting, storing, monitoring and reusing, a part of the excessive kinetic energy during the intended deceleration of the EV [9]. At this deceleration-regenerative phase the electric motor does not consume energy to move the vehicle, instead its role changes to become a generator. The electric energy collected by the regenerative system should be properly stored for later use [10].

A. Supercapacitors

Supercapacitors present the following characteristics, that along with their relative small weight, make them an efficient solution as a regenerative braking energy storage medium and as a source of auxiliary power *bursts* at the EVs.

- They have extremely long shallow-cycle life and are best suited for applications with low energy but high power demand. They, also, do not suffer from degradation due to low temperatures. [10]
- They may be rapidly charged using simple charging methods. They present low internal resistance, have energy densities that are approximately 10% of conventional batteries but their power density is 10-100 times greater [11].

B. Electric Circuit Topology

A variety of topologies is presented at recent works of EVs with regenerative braking system. The most common architecture comprises of the following modules [5], [6], [9], [12]:

- the EV's main electric power source, either a hydrogen fuel cell or rechargeable batteries,
- the regenerative energy storage medium, either SC or rechargeable batteries,
- a charging device to regulate the regenerative electric energy and charge the energy storage medium,
- the vehicle's electric motor operated as generator,
- the electric motor's driver-controller operated as rectifier,
- a set of electronically controllable switches to activate and control the alternative *paths* and *directions* of the

[1] Giannis Tzotrzis is an undergraduate student at the School of Electronic and Computer Engineering of the Technical University of Crete.

[2] Alexandros Amargianos is a graduate student at the School of Production Engineering and Management of the Technical University of Crete.

[3*] corresponding author: Savvas Piperidis is with the Intelligent Systems and Robotics Laboratory, School of Production Engineering and Management of the Technical University of Crete, 73100 Chania, Hellas. spiperidis@isc.tuc.gr

[4] Eftichios Koutroulis is with the Faculty of School of Electronic and Computer Engineering of the Technical University of Crete.

[5] Nikos C. Tsourveloudis is with the Faculty of School of Production Engineering and Management of the Technical University of Crete.

electric energy produced by the regenerative system and consumed by the EV and

- the Regenerative system Embedded Computer (REC).

In [7] an alternative topology is presented: an additional generator, instead of the EV's electric motor, is used to charge SC or batteries. Other alternative architectures use the methods of superconducting magnetic energy storage (SMES) or flywheel energy storage (FES) to accumulate the energy harvested by the regenerative system [13]. SMES uses magnetic field to store and instantly release energy, presenting the advantages of high power density, theoretically infinite number of charge-discharge cycles and efficiency higher than 95% [14], [15]. Its high cost prevents this method to be considered as the ideal solution for shorter duration energy storage applications. The FES method uses a flywheel rotor which is spun by the vehicle's braking action. It offers long lifetimes, an energy efficiency ratio of up to 90% combined with high energy density [16]. The disadvantages of the FES method are the energy losses along with the reliability problems due to friction and mechanical stresses, the potential hazard due to a possible mechanical failure, the relatively poor energy density combined with the relative big weight and the large standby losses [17]–[19].

C. Electronic switches

The switches are a significant part of a regenerative system. They electronically actuate the alternative electric circuits, connecting the main or the secondary-*regenerative* power sources with the electric motor, the generator and the regenerative energy storage medium. Electronic switches are materialized using transistors, relays or contactors. The latter two suffer from mechanical stress and contacts' degradation and thus their operating lifetime is limited to a certain number of switching actions. Their turn on-off delay time is hundred times slower than the transistors. Moreover, they present higher current consumption in comparison to a transistor acting as an electronic switch, especially in low current flow values.

D. The TUCer-14 Case Study

Fig. 1. The TUCer-14 prototype urban concept vehicle

The proposed regenerative system was designed to operate as a part of the electrical propulsion system of the TUCer-14

EV [20], Fig. 1. The vehicle utilizes a hydrogen fuel cell and a SC bank, charged via the regenerative system, as primary and auxiliary energy sources respectively. It is a single seater, prototype urban concept vehicle, designed to participate in low consumption competitions. Instead of many recent works on regenerative braking that rely on simulation or laboratory testing [5], [6], [9], [13], [17], [21], the proposed system was designed, developed and tested on the road, in real world conditions. It follows specifications that comply with *hard* restrictions regarding efficiency, reliability and dimensions. Moreover, it is able to operate in a *plug and play* manner and be easily added or removed from the vehicle's powertrain according to the specific driving conditions of each competition. Finally the control algorithm of the system's controller is implemented by a sequential Finite State Machine (FSM) offering great potentials for expansion, easy maintenance and debugging while at the same time it remains extremely simple and straightforward.

The rest of the paper is organized in four sections. Section II analyses the basic design of the regenerative system including the descriptions of the basic system's module. Section III describes the control methodology used to develop the embedded computer controller program. Section IV refers to the experimental results of the on-road testings and Section V argues about the conclusions of the proposed work and states about the future plans.
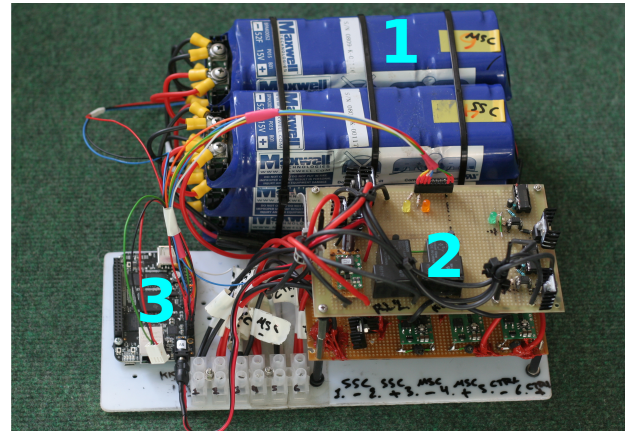
II. DESIGN CONCEPTS

Fig. 2. The regenerative system. (1) supercapacitors bank, (2) buck converter and MOS-FETs, (3) single board embedded computer.

The TUCer-14 regenerative system comprises of the following modules, Fig. 2, 3:

1) a 15V-312F SC bank acting as the regenerative energy repository,
2) a Buck-Converter (BC) for the charging of the SC,
3) the vehicle's three phase brushless electric motor and its electronic driver-controller operating as generator and rectifier, respectively, during the regeneration phase,
4) a contactor and a set of Metal-Oxide Semiconductor Field-Effect Transistors (MOS-FETs) operating as electronically controlled switches and

5) a single board embedded computer implementing the regenerative control procedure.

An important system's characteristic is its autonomy, in the sense of powering its electronics by its own SC bank. There is no need for connection to external power or ground signals. Instead, the whole system may operate in a *plug and play* manner, just by connecting it between the main power supply and the electric motor driver of the EV. The regenerative system's total dimensions are $25 \times 14 \times 28$cm and its total weight is 3.4kg.

A. Supercapacitors

The SC bank consists of six Maxwell BPAK0052 P015 B01 packs in parallel [22]. Each one of these packs has nominal capacitance 52F, rated voltage 15V, equivalent series resistance (ESR) 0.8mΩ and maximum continuous current 20A, resulting to a total bank capacitance of 312F at 15V and a total ESR of 0.133mΩ. The choice of SC instead of the other storage mediums, depicted at the previous section, was made due to the following reasons:

- The relative small bank dimensions of $13 \times 20 \times 11$cm and weight of 3kg.
- The adequate power and energy provided when the bank is fully charged. The vehicle may easily start moving and drive a few hundred meters when powered exclusively from the SC auxiliary power source.
- The SC have extremely low ESR and may be instantaneously charged using the BC or provide sufficient bursts of power during discharging.
- The SC theoretically may operate for an infinite number of charge-discharge cycles.
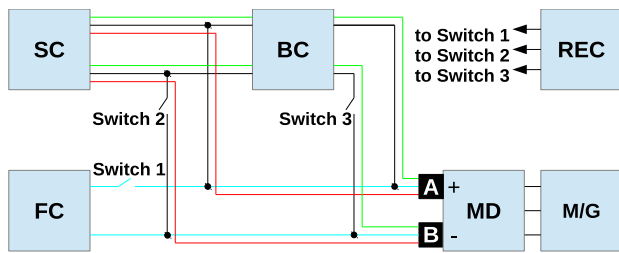
B. Buck Converter

Fig. 3. The architecture of the proposed regenerative system: **Switch 1, 2** and **3** activate the fuel cell (light blue), discharge SC (red) and charge SC (green) operation modes respectively, **FC** is the hydrogen fuel cell, the vehicle's main power source, **SC** is the supercapacitors bank, the vehicle's auxiliary power source, **BC** is the buck converter used to charge the SC, **MD** is the electric motor's driver operating, also, as a rectifier during the regenerative phase, **M/G** is the vehicle's 3-phase motor operating, also, as a generator during the regenerative phase, **REC** is the regenerative system's embedded computer that hosts the control processes and **A-B** are the motor driver's inputs or, during the regenerative phase, rectifier's outputs.

During the deceleration of the vehicle the three-phase electric motor and its driver circuit operate as generator and rectifier respectively and the terminals A-B in Fig. 3 produce unregulated voltage. Due to the extremely low RES of the SC, it is necessary to connect their bank via a switch-mode

charger device to the regenerative current output of the A-B terminals [23] to avoid a short circuit.

The unregulated voltage and current of the regenerative electricity depends on the vehicle's velocity during the deceleration. This fact may result in excessive current flows from the generator to the SC via the rectifier along with voltage values much higher than the SC bank rated voltage that will potentially destroy the rectifier, the motor or both of them.

The BC, employed between the rectifier and the SCs bank, eliminates the above undesired conditions during charging process and protects the system's reliability. It operates as a voltage source tuned to output the rated voltage of the SC bank. The regenerative current is analogous to the potential difference between the input voltage of the BC and the instant voltage of the SC bank. Thus, as the voltage of the SC bank increases during the regenerative process, the charging current decreases.

C. Electronic Switches

TABLE I
SWITCHES' STATE AND MODES OF OPERATION

| | | mode | | |
		charging SC	discharging SC	FC operation
switch	switch 1	●	○	○
	switch 2	○	●	○
	switch 3	○	○	●

The vehicle's electric powertrain may operate in three distinct, mutually exclusive modes.

Fuel cell operation: the vehicle is accelerating or moving with constant speed using the fuel cell as its main power source.

Charging SC: the vehicle is deliberately decelerating, charging the SC bank via the regenerative system.

Discharging SC: the vehicle is accelerating or moving with constant speed using the electric energy stored at the SC.

To implement the commutation between the above modes three switches are used, Fig. 3. Each time, the regenerative system controller program allows only one of them to be at the *turned on* position. Table I summarizes the allowed switches' configuration and for each one of them shows the respective mode of system's operation. The ● and the ○ signs correspond to a switch operating at the *turn on* or *turn off* position respectively. For safety reasons, the fuel cell is equipped with an output contactor controlled by its own embedded computer. This is the *Switch 1*, Fig. 3, also used by the REC to implement the *fuel cell operation* mode. On the other hand SC discharging and charging operations are handled by *Switch 2* and *Switch 3* MOS-FETs, Fig. 3, operating as switches because of their advantages referenced at the previous section. Studying their power consumption during, for example, a typical discharge mode operation of the system, the mean current value flowed from the SC bank is approximately 4.5A and the power consumption of *Switch*

2 is 0.15W [24]. If a power relay was used as a switch instead of the MOS-FET, then the power consumption on its coil and contact resistance would be 1.32W [25].

D. Embedded Computer

The regenerative controller program is running on the BeagleBone Black [26], an Arm-A8, low power, small factor embedded single board computer, powered by the open source Debian operating system [27]. With dimensions 8.6×5.3cm, weight 0.04kg and a power consumption of 2W BeagleBone Black is an attractive solution as a processing unit for the TUCer-14 regenerative system.
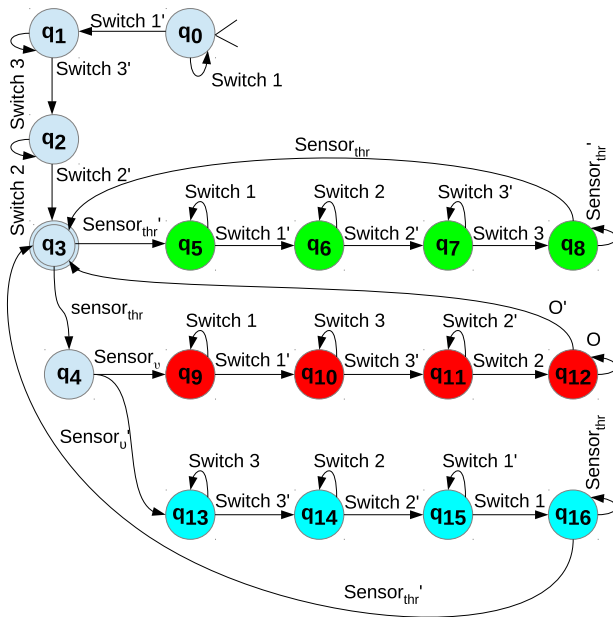
III. CONTROL METHODOLOGY

Fig. 4. Controller program's Finite State Machine. The three different colours depict the three different system's operation modes: light blue for the operation with the FC as main power source, green for the charging SC mode and red for the discharging SC mode.

The regenerative system's controller program is based on an FSM used as a computational model consisting of a set of states and transitions. This is a dynamic approach that describes the evolution over time of a set of discrete and continuous state variables. Controller program's FSM can be described as the tuple $A = (Q, \Sigma, \delta, q_0, F)$ [28], where:

- $Q = \{q_0, q_1, \ldots, q_{16}\}$ is the finite set of states, described in Table II. In Fig. 4 the light blue (FC is the main power source), red (discharging SC) and green (charging SC) colours in states' figure indicate the system's operation mode.
- Σ is the the alphabet, consisting of a finite set of symbols explained in Table III and shown in Fig. 4.
- δ: $Q \times \Sigma \to Q$ is the state transition function described in Table IV and Fig. 4. The Table IV defines for every state in the first column the resulting state for the alternative inputs in the second and third columns.
- $q_0 \in Q$ is the initial state of the FSM.

- $F = \{q_3\}$ is the set of final states.

The FSM technique was chosen as the REC control strategy representation because of its advantages described bellow:

1) It produces an object-oriented depiction of the system, easily translated to a controller program using an object oriented programming language. The REC controller program was developed in C++.
2) The definition of Q, Σ and δ finite sets is a strict but at the same time straightforward method helping error elimination and debugging.
3) It is intuitive and easily conceivable, even for someone with less or none knowledge for the system.
4) It is less extensive and complicated than the other representation and programming techniques, like the algorithm or the flow chart.
5) The FSM technique provides the ability of making changes to the system by adding or removing states or transitions or both of them.
6) It is best suited to systems with sequential logic, like the one described at this paper.
7) There are methods for FSM optimization by minimizing the Q and δ sets [28].

The three first FSM states, $q_0 \ldots q_2$ represent the hardware initialization phase, during the regenerative system's start up process and ensure that all switches are turned off. Afterwards, there are three, mutually exclusive, paths corresponding to the three system operating modes: the operation with the FC as main power source, the charging and the discharging of the SC - light blue, green and red paths respectively at Fig. 3, 4. Each one of these paths implements the sequential control of the electronic switches mentioned in Table I. The q_3 is the FSM's final state and also represents the idle condition in which the system returns after every possible operation. The regenerative system utilizes two sensors. The first is used as a throttle switch and senses whether the driver presses the acceleration pedal or not. The second estimates the SC state of charge by comparing the voltage value of the SC bank with a given threshold. With respect to the description of the FSM transitions in Table IV, the throttle sensor value corresponds to the $Sensor_{thr}$ transitions, while the comparison between the SC bank voltage and the given threshold corresponds to the $Sensor_v$ transitions.

When the throttle switch is turned on (transition $Sensor_{thr}$), meaning the driver wants to accelerate, the system is transitioned to q_4–*Selecting energy source*. From q_4, depending on the state of charge of the SC bank, the system operates with the FC as the main power source (if the SC bank is not charged–transition $Sensor_v$´ –light blue colour path) or with the SC bank as auxiliary power source (if the SC bank is charged–transission $Sensor_v$–red colour path). When the system is at the discharge SC mode and the driver releases the throttle *OR* the SC bank's state of charge is lower than the given threshold (transition O´), then the system returns to the q_3 state. When the system operates with the FC as the main power source and the driver releases the

throttle (transition $Sensor_{thr}´$), then the system returns to the q_3 state, as well.

If the throttle switch is turned off, meaning the driver wants to decelerate, (transition $Sensor_{thr}´$) then the charging SC mode is activated (green colour path). When the system is at the charge SC mode and the driver presses the throttle (transition $Sensor_{thr}$) then the system returns to the q_3 state, otherwise the SC charging continues (transition $Sensor_{thr}´$).

TABLE II

DESCRIPTION OF FSM'S STATES

State	State Description
q_0	*Initializing system* - waiting for Switch 1 to turn off
q_1	*Initializing system* - waiting for Switch 3 to turn off
q_2	*Initializing system* - waiting for Switch 2 to turn off
q_3	Stand by - idle
q_4	Selecting energy source
q_5	*Charging SC mode*–waiting for Switch 1 to turn off
q_6	*Charging SC mode*–waiting for Switch 2 to turn off
q_7	*Charging SC mode*–waiting for Switch 3 to turn on
q_8	*Charging SC mode*–Charging SC
q_9	*Discharging SC mode*–waiting for Switch 1 to turn off
q_{10}	*Discharging SC mode*–waiting for Switch 3 to turn off
q_{11}	*Discharging SC mode*–waiting for Switch 2 to turn on
q_{12}	*Discharging SC mode*–using SC as auxiliary power source
q_{13}	*FC power source mode*–waiting for Switch 3 to turn off
q_{14}	*FC power source mode*–waiting for Switch 2 to turn off
q_{15}	*FC power source mode*–waiting for Switch 1 to turn on
q_{16}	*FC power source mode*–FC is the main power source

TABLE III

DESCRIPTION OF FSM'S ALPHABET

Symbol	Symbol Description
Switch 1	Switch 1 (FC) is turned on
Switch 1´	Switch 1 (FC) is turned off
Switch 2	Switch 2 (discharging SC) is turned on
Switch 2´	Switch 2 (discharging SC) is turned off
Switch 3	Switch 3 (charging SC) is turned on
Switch 3´	Switch 3 (charging SC) is turned off
$Sensor_v$	SC's voltage more than specified threshold
$Sensor_v´$	SC's voltage less than specified threshold
$Sensor_{thr}$	Throttle is turned on
$Sensor_{thr}´$	Throttle is turned off
O	$Sensor_v$ AND $Sensor_{thr}$
O´	$Sensor_v´$ OR $Sensor_{thr}´$

IV. EXPERIMENTAL TESTING

The proposed regenerative braking system was developed and tested on-road using the prototype urban concept TUCer-14 EV. The testing took place in the Technical University of Crete campus at Chania, Hellas. The route followed is shown in Fig. 5 and can be divided in 4 sections-tracks:

- The vehicle accelerates from the starting point, approaching the parking CP1 and stopping at its entrance-exit (red track, 0.22km, slight downhill).
- Starting from CP1 entrance-exit, the vehicle drives around the parking with one instant stop at the half of the route. It finally stops at the CP1 entrance-exit (green track, 0.33km, flat).

TABLE IV

TRANSITION TABLE

| Current state	Next state, Input	Next State, Input
q_0	q_0, Switch 1	q_1, Switch 1´
q_1	q_1, Switch 3	q_2, Switch 3´
q_2	q_2, Switch 2	q_3, Switch 2´
q_3	q_4, $Sensor_{thr}$	q_5, $Sensor_{thr}´$
q_4	q_9, $Sensor_v$	q_{13}, $Sensor_v´$
q_5	q_5, Switch 1	q_6, Switch 1´
q_6	q_6, Switch 2	q_7, Switch 2´
q_7	q_7, Switch 3´	q_8, Switch 3
q_8	q_8, $Sensor_{thr}´$	q_3, $Sensor_{thr}$
q_9	q_9, Switch 1	q_{10}, Switch 1´
q_{10}	q_{10}, Switch 3	q_{11}, Switch 3´
q_{11}	q_{11}, Switch 2´	q_{12}, Switch 2
q_{12}	q_{12}, O	q_3, O´
q_{13}	q_{13}, Switch 3	q_{14}, Switch 3´
q_{14}	q_{14}, Switch 2	q_{15}, Switch 2´
q_{15}	q_{15}, Switch 1´	q_{16}, Switch 1
q_{16}	q_{16}, $Sensor_{thr}$	q_3, $Sensor_{thr}´$
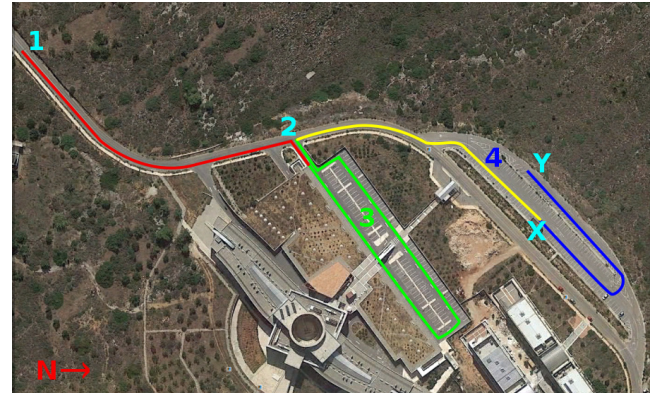
Fig. 5. The regenerative braking testing route inside the university campus. (1) Starting point, (2) first campus parking entrance-exit, (3) first campus parking CP1, (4) second campus parking CP2.

- Starting from CP1 entrance-exit, the vehicle approaches the CP2 parking and stops at the point X (yellow track, 0.175km, slight downhill).
- The vehicle is driven inside CP2 parking, from the point X to the point Y (blue track, 0.169km, flat).

The red and yellow tracks were driven with a speed up to 30km/h while the green and blue tracks were driven with 10km/h due to the university campus speed limits for the urban and parking premises. The tracks and the driving speeds are a typical example of the urban driving routine: low speed values and recurring stop-and-go events. To gather experimental results and evaluate the regenerative system, the TUCer-14 EV was driven in the above tracks twice: firstly, without the regenerative system, using the FC as the only power source and secondly with the regenerative system activated using both the FC and the SC bank as main and auxiliary power sources respectively. The driving conditions were controlled to be as same as possible between the two consecutive test drives. The vehicle accelerates with a pre-programmed acceleration ramp and uses electronic speed control to maintain a given speed.

A. Experimental Data

Figure 6 presents the speed profile of the tests and Fig. 7 shows the voltage and current values at the terminals A-B of the motor driver shown in Fig. 3. Figure 8 shows the electric power consumed by the electric motor. At the test drive with the FC as the only power source for the electric motor the voltage values, shown in Fig. 7 vary between 45-28V. When the regenerative system is activated, then the voltage values drop below 15V as either the system charges the SC bank during deceleration (for example from the 11th until the 46th second) or powers the electric motor via the auxiliary power of the charged SC (from the 212th until the 280th second).
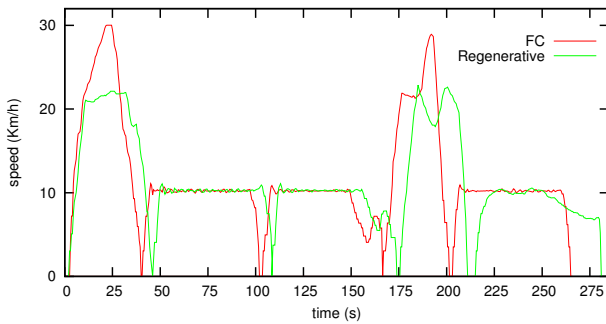

Fig. 6.   Speed profiles during the test drives.

1) Red Track: At the start of the test drive the vehicle starts accelerating and reaches the speed of 20 km/h at the 9th second, Fig. 6. Then the driver releases the acceleration pedal and the vehicle rolls the slight downhill until the entrance-exit of the CP1. When the regenerative system was not enabled (Fig. 6 red graph), the vehicle's momentum accelerated it up to 30km/h (22th second). On the other hand, when the regenerative system was enabled (Fig. 6 green graph), the vehicle's top speed, until reaching CP1 entrance-exit, is limited to 21.4km/h. This is ought to the additional drag force due to the generator operation that converts a part of the vehicle's kinetic energy to electricity stored in the SC bank (from the 10th until the 46th second). The lower speed valuess during deceleration with the regenerative system activated, explain the time deviation between the two graphs in the figures. At the entrance of CP1 the vehicle stops.

2) Green Track: The vehicle starts from the entrance of CP1 and drives around the parking with a speed of 10km/h, performs one instant stop at the half of the track and finally stops at the CP1 exit. At this track the motor consumes energy from the FC in both test drives.

3) Yellow Track: The vehicle accelerates until the 184th second when it reaches the speed of 20km/h, then the driver releases the acceleration pedal and the vehicle rolls the slight downhill until the point X, where it performs an instant stop. At the test drive with the regenerative system activated, the SC bank is charged during the period from the 185th until the 211th second.

4) Blue Track: Inside the CP2 the vehicle accelerates to a speed of 10km/h and after 54s it finally stops at the point
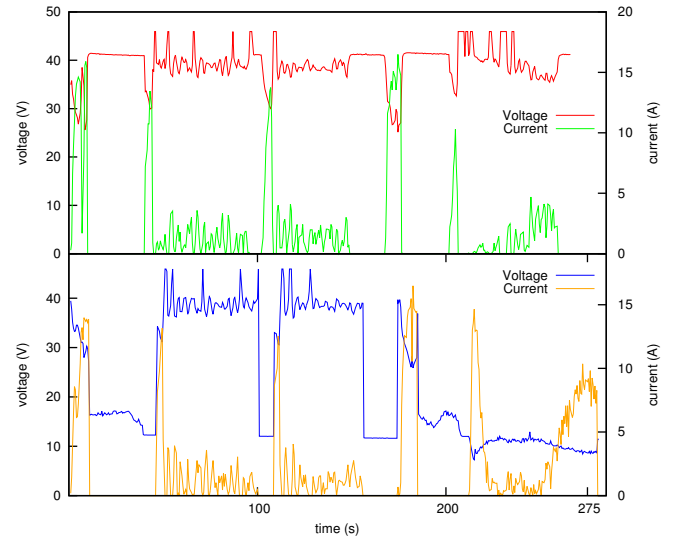

Fig. 7.   Voltage and current at the motor driver/rectifier terminals. At the top figure the regenerative system was not activated.
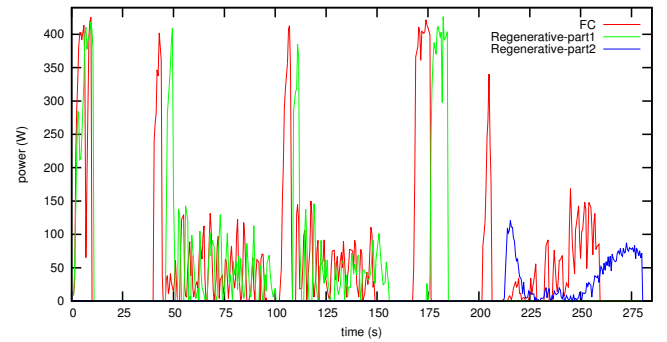

Fig. 8.   Power consumption with and without regenerative braking. The green graph (regenerative-part1) corresponds to the power consumption during the test with the regenerative system activated until the 212th second when the vehicle enters the blue track. The blue graph (regenerative-part2) corresponds to the power consumption when the vehicle uses the auxiliary SC bank as power source at the blue track.

Y. At the test drive with the regenerative system the motor is powered from the SC bank during this track, as shown at the blue graph of Fig. 8.

B. Results

During the test drive with the regenerative system activated at the TUCer14 vehicle, the SC bank is charged during the periods from the 10th until the 46th and from the 185th until the 211th second. The charged SC operate as the vehicle's auxiliary power source from the 212th second until the end of the test and offer 2482J. This is the gain from the regenerative system operation, at a test drive scenario that consumed in total 15322J. At the test drive that the fuel cell was operating as the only power source, the energy consumed at the same blue track was 3073J. This difference is explained because of the different specifications of the two power sources. The FC loses its efficiency whenever it has

to encounter sudden load rises, like the one at the blue track start from the 202th until the 206th second. On the contrary, the SC bank behaves much more efficiently at this kind of situations.

V. CONCLUSIONS AND FURTHER WORK

A compact regenerative system for EVs was developed and tested at the TUCer-14 prototype. The main advantages of the system is its compact design and the plug-and-play philosophy. Its control strategy consists of a simple set of rules applied on data provided by the two system's sensors. The combination of this control system with the hardware of MOS-FETs, SCs and buck converters results to an integrated regenerative braking system operating in three individual, mutually exclusive modes: charging, discharging and FC-operation. On-road testing proved the reliability and the efficiency of the system on a prototype EV.

Future plans include several modifications that will potentially improve the regenerative system's efficiency:

- The ability from both SC and FC to power the system in the same time connected in parallel, is an issue already under consideration. The SC may counterbalance the disadvantages of the FC efficiency, like for example during sudden rises of the load.
- The SC bank may be charged, not only via the generator during the vehicle's deceleration, but also from the FC during. This could exploit the periods when the vehicle is stopped, in a standby mode and then the FC could efficiently charge the SCs.
- The control procedure could be more *intelligent*, taking into account data, not only from the SC voltage and the throttle switch, but also from the vehicle's speed, the desired driving policy or the amount of fuel left inside the tank.

REFERENCES

[1] A. Pina, P. Baptista, C. Silva, and P. Ferro, "Energy reduction potential from the shift to electric vehicles: The Flores island case study," *Energy Policy*, vol. 67, no. 0, pp. 37 – 47, 2014.

[2] C. Ziogou, D. Ipsakis, P. Seferlis, S. Bezergianni, S. Papadopoulou, and S. Voutetakis, "Optimal production of renewable hydrogen based on an efficient energy management strategy," *Energy*, vol. 55, no. 0, pp. 58 – 67, 2013.

[3] Melody L. Baglione, "Development of system analysis methodologies and tools for modeling and optimizing vehicle system efficiency," Ph.D. dissertation, University of Michigan, 2007.

[4] Ali Emadi, *Energy - Efficient Electric Motors*. New York: Marcel Dekker, 2005.

[5] Qi Li and Weirong Chen and Yankun Li and Shukui Liu and Jin Huang, "Energy management strategy for fuel cell/battery/ultracapacitor hybrid vehicle based on fuzzy logic," *International Journal of Electrical Power & Energy Systems*, vol. 43, no. 1, pp. 514 – 525, 2012.

[6] M. Mohammedi, O. Kraa, M. Becherif, A. Aboubou, M. Ayad, and M. Bahri, "Fuzzy logic and passivity-based controller applied to electric vehicle using fuel cell and supercapacitors hybrid source," *Energy Procedia*, vol. 50, no. 0, pp. 619 – 626, 2014, technologies and Materials for Renewable Energy, Environment and Sustainability (TMREES14 EUMISD).

[7] B. H. Kim, O. J. Kwon, J. S. Song, S. H. Cheon, and B. S. Oh, "The characteristics of regenerative energy for pemfc hybrid system with additional generator," *International Journal of Hydrogen Energy*, vol. 39, no. 19, pp. 10 208 – 10 215, 2014.

[8] P. Clarke, T. Muneer, and K. Cullinane, "Cutting vehicle emissions with regenerative braking," *Transportation Research Part D: Transport and Environment*, vol. 15, no. 3, pp. 160 – 167, 2010.

[9] R. Teymourfar, B. Asaei, H. Iman-Eini, and R. N. fard, "Stationary super-capacitor energy storage system to save regenerative braking energy in a metro line," *Energy Conversion and Management*, vol. 56, no. 0, pp. 206 – 214, 2012.

[10] E. Karden, S. Ploumen, B. Fricke, T. Miller, and K. Snyder, "Energy storage devices for future hybrid electric vehicles," *Journal of Power Sources*, vol. 168, no. 1, pp. 2 – 11, 2007.

[11] P. Sharma and T. Bhatti, "A review on electrochemical double-layer capacitors," *Energy Conversion and Management*, vol. 51, no. 12, pp. 2901 – 2912, 2010.

[12] L. Sun and N. Zhang, "Design, implementation and characterization of a novel bi-directional energy conversion system on {DC} motor drive using super-capacitors," *Applied Energy*, no. 0, pp. –, 2014.

[13] G. Ren, G. Ma, and N. Cong, "Review of electrical energy storage system for vehicular applications," *Renewable and Sustainable Energy Reviews*, vol. 41, no. 0, pp. 225 – 236, 2015.

[14] P. J. Hall and E. J. Bain, "Energy-storage technologies and electricity generation," *Energy Policy*, vol. 36, no. 12, pp. 4352 – 4355, 2008, foresight Sustainable Energy Management and the Built Environment Project.

[15] A. Morandi, L. Trevisani, F. Negrini, P. Ribani, and M. Fabbri, "Feasibility of superconducting magnetic energy storage on board of ground vehicles with present state-of-the-art superconductors," *Applied Superconductivity, IEEE Transactions on*, vol. 22, no. 2, pp. 5 700 106– 5 700 106, April 2012.

[16] Daberkow, Andreas and Ehlert, Marcus and Kaise, Dominik, "Electric car operation and flywheel energy storage," in *Conference on Future Automotive Technology*, M. Lienkamp, Ed. Springer Fachmedien Wiesbaden, 2013, pp. 19–30.

[17] R. Sebastián and R. P. Alzola, "Flywheel energy storage systems: Review and simulation for an isolated wind power system," *Renewable and Sustainable Energy Reviews*, vol. 16, no. 9, pp. 6803 – 6813, 2012.

[18] R. Walawalkar, J. Apt, and R. Mancini, "Economics of electric energy storage for energy arbitrage and regulation in new york," *Energy Policy*, vol. 35, no. 4, pp. 2558 – 2568, 2007.

[19] *Handbook of Energy Storage for Transmission or Distribution Applications*, EPRI, Palo Alto, CA, 2002, 1007189.

[20] TUC Eco Racing Team. (2015, February) Technical University of Crete. [Online]. Available: http://www.tucer.tuc.gr

[21] S. H. Kim, O. J. Kwon, D. Hyon, S. H. Cheon, J. S. Kim, B. H. Kim, S. T. Hwang, J. S. Song, M. T. Hwang, and B. S. Oh, "Regenerative braking for fuel cell hybrid system with additional generator," *International Journal of Hydrogen Energy*, vol. 38, no. 20, pp. 8415 – 8421, 2013.

[22] Maxwell Technologies, *BC BPAK Power Series 15v BOOSTCAP Ultracapacitors*, 2010. [Online]. Available: http://www.maxwell.com

[23] Maxwell Technologies, *Charging of Ultracapacitors*, 2005. [Online]. Available: http://www.maxwell.com

[24] STMicroelectronics, *STP75NF75 STripFETTM II Power MOSFET*, 2007. [Online]. Available: http://www.st.com

[25] OMRON Electronics, INC, *G8P Power PCB Relay*.

[26] BeagleBoard Foundation. (2015, February) BeagleBone Black. [Online]. Available: http://beagleboard.org/black

[27] Debian Project. (2015, February) Debian, the universal operating system. [Online]. Available: https://www.debian.org/

[28] Z. Kohavi and N. Jha, *Switching and Finite Automata Theory*. Cambridge University Press, 2010.